International Journal of Mechanical, Industrial and Aerospace Sciences
ISSN: 2517-9950
Vol:7, No:2, 2013

Compliance Modelling and Optimization of Kerf during WEDM of Al7075/SiC_P Metal Matrix Composite

Thella Babu Rao, A. Gopala Krishna

***Abstract*—**This investigation presents the formulation of kerf (width of slit) and optimal control parameter settings of wire electrochemical discharge machining which results minimum possible kerf while machining Al7075/SiC_P MMCs. WEDM is proved its efficiency and effectiveness to cut the hard ceramic reinforced MMCs within the permissible budget. Among the distinct performance measures of WEDM process, kerf is an important performance characteristic which determines the dimensional accuracy of the machined component while producing high precision components. The lack of available of the machinability information such advanced MMCs result the more experimentation in the manufacturing industries. Therefore, extensive experimental investigations are essential to provide the database of effect of various control parameters on the kerf while machining such advanced MMCs in WEDM. Literature reviled the significance some of the electrical parameters which are prominent on kerf for machining distinct conventional materials. However, the significance of reinforced particulate size and volume fraction on kerf is highlighted in this work while machining MMCs along with the machining parameters of pulse-on time, pulse-off time and wire tension. Usually, the dimensional tolerances of machined components are decided at the design stage and a machinist pay attention to produce the required dimensional tolerances by setting appropriate machining control variables. However, it is highly difficult to determine the optimal machining settings for such advanced materials on the shop floor. Therefore, in the view of precision of cut, kerf (cutting width) is considered as the measure of performance for the model. It was found from the literature that, the machining conditions of higher fractions of large size SiC_P resulting less kerf where as high values of pulse-on time result in a high kerf. A response surface model is used to predict the relative significance of various control variables on kerf. Consequently, a powerful artificial intelligence called genetic algorithms (GA) is used to determine the best combination of the control variable settings. In the next step the conformation test was conducted for the optimal parameter settings and found good agreement between the GA kerf and measured kerf. Hence, it is clearly reveal that the effectiveness and accuracy of the developed model and program to analyze the kerf and to determine its optimal process parameters. The results obtained in this work states that, the resulted optimized parameters are capable of machining the Al7075/SiC_P MMCs more efficiently and with better dimensional accuracy.

***Keywords*—**Al7075SiC_P MMC, kerf, WEDM, optimization.

Thella Babu Rao is Assistant Professor at the Department of Mechanical Engineering, GITAM University, Hyderabad, Andhra Pradesh, India, PIN – 502 329, (e-mail: baburao_thella@yahoo.co.in).

A Gopala Krishna is Professor at the Department of Mechanical Engineering, University College of Engineering, Jawaharlal Nehru Technological University, Kakinada, PIN - 533 003, Andhra Pradesh, India. (e-mail: dr.a.gopalakrishna@gmail.com).

I. Introduction

METAL matrix composites have found many applications in the present high speed aerospace and automobile industries. These are classified as advanced materials due to the improved properties of high strength-to-weight ratio, excellent wear resistance, lower coefficient of thermal expansion and capability to work at elevated temperatures [1]. Industries are producing these MMCs using several methods such as powder metallurgy, uni-axial pressing, iso-static pressing, extrusion, spray forming, stir-casting, rheo-casting, and compo-casting. However, due to the presence of the discontinuously dispersed hard ceramic, machining of these materials became challenge for the manufacturing industries today. Due to this MMCs as categorized as highly difficult-to-cut materials and converged their applications to limited and peculiar components only.

Since, a number of factors like chemical compositions, ceramic reinforcement and its distribution, processing rout and the processing conditions are highly significant on the machinability of MMCs. The use of conventional machining methods like turning, milling, drilling are found as uneconomical due to the severe tool wear due to the presence of hard ceramic content [2], [3]. However, the non-conventional machining method like laser beam machining (LBM), plasma cutting, electron beam machining (EBM) are being used in the industries to cut these composites, but are identified as highly costlier and required complicated equipment in their operation. On the other hand, electric discharge machining (EDM) became popular method for its efficiency and cost effectiveness to machine these composites. But it is limited to produce simple contours on the machined part and also required elaborate preparation for pre-shaped electrode as tool to get the required contours over the component.

Subsequently, wire electrical discharge machining (WEDM) as non-contact type machining method is proven as an economical and efficient method for machining metal matrix composites into complex contours [4], [5]. In its working principle, WEDM is a thermo-electrical process in which the metal removal takes place by a series of discharges of electric sparks at the interface of continuously supplied and directed wire (electrode) and the work piece in the presence of dielectric medium. The control parameters like discharge current, pulse-on time, pulse-off time, and voltage are most common significant for high speed machining of WEDM [6], [7]. While in the case of machining metal matrix composites,

the variables like volume fraction and particulate size has considerable effect on the performance of the WEDM. Usually, the manufacturers of the WEDM machines provides the database of electrode materials and the operational details and process control variables for most regularly used materials only. The information provided by the manufactures of WEDM is not adequate for machining such advanced materials. Hence, the database of feasible control variables of WEDM for machining MMCs could widen their applications in industries. One of the most significant performance characteristics of WEDM process is kerf. The kerf determines the dimensional accuracy of the machined component. According to Aniza et al. [8] investigation on WEDM, the increased feed rate increases the kerf and also caused to inaccuracies in the kerf [9]. Sangju Lee et al. [10] found that, the reason decreased kerf at higher feed rate is due to less lateral discharge energy. The electrical parameters like voltage and pulse duration are highly significant factors on kerf [11]. Therefore, an extensive experimental work is needed to completely understand the individual and interactive effects of various WEDM control parameters. This investigation aimed to provide the empirical model to predict the kerf (Kw) in terms of the most significant WEDM control parameters for Al7075/SiCP MMC using response surface methodology (RSM) and to find the optimal control variables which machine the composite with minimum possible kerf using genetic algorithms (GA).

II. Experimental Procedure

The robust Taguchi's design of experiments (DOE) is employed to minimize the number of experimental runs and the experiments are designed for L_{27} orthogonal array consists of 27 experimental runs [12]. Then the machining was conducted on a five-axis CNC-Wire Electrical Discharge Machine, Model Number CT 520A, made by Joemars Machinery and Electric Industrial Co.Ltd., Taiwan. SiC_P reinforced Al7075 metal matrix composites are used as work pieces for machining. These MMCs are produced by stir casting rout. The MMCs are produced with different particulate sizes as 25, 50 and 75µm reinforced each at distinct volume fractions as 5, 10 and 15%. The details of work specimens, electrode and the other machining conditions are listed in Table I. Pulse-on time, pulse-off time and wire tension were selected as WEDM process parameters in addition to the composite variables of particulate size and volume fraction of SiC_p. The levels of process variables are selected based on the literature and the pilot experiment as listed Table II. The design of experimental matrix presented in Table III.

TABLE I
Machining Conditions

S. No.	Description
1	Work piece (anode) : Al7075/SiC_p
2	Tool (cathode) : Brass wire of diameter 250 µm
3	Work piece height: 6 mm
4	Cutting length: 75 mm
5	Angle of Cut: Vertical
6	Location of work piece : centre to the table
7	Servo reference voltage : 35V
8	Average voltage gap maintained: 40V
9	Die-electric temperature: 25°C
10	Die-electric fluid: Distilled water

TABLE II
Control Factors and Their Levels

S. No.	Variable	Notation	Levels		
			1	2	3
1	Particulate size (µm)	X_1	25	50	75
2	Volume of SiC (%)	X_2	5	10	15
3	Pulse-on Time (µs)	X_3	6	8	10
4	Pulse-off Time (µs)	X_4	25	35	45
5	Wire tension (gms)	X_5	1	5	9

After each experiment, kerf of the machined work piece was measured by using Computerised Optical Microscope, model GX51 inverted microscope made by OLYMPUS CORPORATION with the magnification range of 200µm.

Fig. 1 Experimental setup for kerf measurement

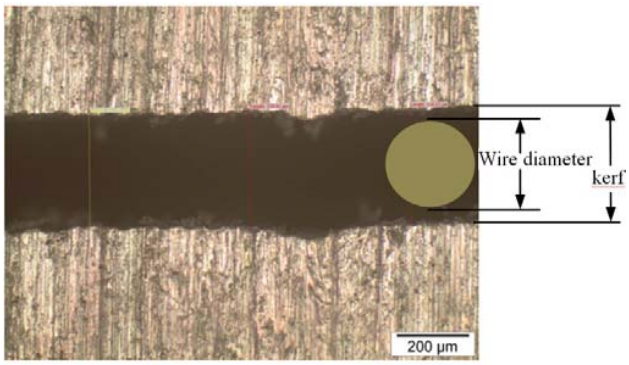

Fig. 2 Top viwe of the kerf and wire diameter

Kerf at three different locations along the machined length in perpendicular direction is measured and the averages of them were considered as the Kw and are listed in Table III. Fig. 1 shows the experimental setup used to measure the

response kerf and the Fig. 2 represents the kerf width of the machined components.

TABLE III
DESIGN OF EXPERIMENTAL MATRIX: TAGUCHI'S L_{27} ORTHOGONAL ARRAY

Exp No.	Coded control factor					Response
	X_1	X_2	X_3	X_4	X_5	Kerf(mm)
1	1	1	1	1	1	0.305
2	1	1	2	2	2	0.359
3	1	1	3	3	3	0.389
4	1	2	1	2	2	0.311
5	1	2	2	3	3	0.341
6	1	2	3	1	1	0.347
7	1	3	1	3	3	0.301
8	1	3	2	1	1	0.324
9	1	3	3	2	2	0.341
10	2	1	1	2	3	0.331
11	2	1	2	3	1	0.338
12	2	1	3	1	2	0.362
13	2	2	1	3	1	0.282
14	2	2	2	1	2	0.331
15	2	2	3	2	3	0.343
16	2	3	1	1	2	0.311
17	2	3	2	2	3	0.318
18	2	3	3	3	1	0.318
19	3	1	1	3	2	0.304
20	3	1	2	1	3	0.331
21	3	1	3	2	1	0.334
22	3	2	1	1	3	0.312
23	3	2	2	2	1	0.314
24	3	2	3	3	2	0.323
25	3	3	1	2	1	0.285
26	3	3	2	3	2	0.300
27	3	3	3	1	3	0.325

III. POSTULATION OF MODEL

The experimental measurements at each run are used to develop the mathematical model based on response surface methodology. This model relates the considered kerf with various control variable settings during machining Al7075/SiC_P. WEDM is such a complex process that interaction effects of the control variables are more significant on machining performances. Therefore the second order polynomial models are fitted for the output responses in terms of the coded variables. The postulated model can be represented in terms of regression coefficients as:

$$\begin{aligned} Kw = {} & 0.33 - 0.0099x_1 - 0.013x_2 + 0.019x_3 - 0.0042x_4 \\ & + 0.0064x_5 - 0.0019x_1^2 + 0.0038x_2^2 - 0.0049x_3^2 \\ & + 0.0002x_4^2 - 0.0036x_5^2 + 0.0047x_1x_2 - 0.0041x_1x_3 \\ & - 0.0029x_1x_4 - 0.0024x_1x_5 - 0.0026x_2x_3 - 0.0065x_2x_4 \\ & - 0.0025x_2x_5 + 0.0009x_3x_4 - 0.0053x_3x_5 + 0.0012x_4x_5 \end{aligned} \quad (1)$$

In the above equation x_1, x_2, x_3, x_4 and x_5 represent the logarithmic transformations for the control factors, particulate size, volume of particulate, pulse-on time, pulse-off time and wire tension respectively and they are given below:

$$x_1 = \frac{\ln(X_1) - \ln(50)}{\ln(75) - \ln(50)}; x_2 = \frac{\ln(X_2) - \ln(10)}{\ln(15) - \ln(10)}; x_3 = \frac{\ln(X_3) - \ln(7)}{\ln(9) - \ln(7)};$$
$$x_4 = \frac{\ln(X_4) - \ln(35)}{\ln(45) - \ln(35)}; x_5 = \frac{\ln(X_5) - \ln(5)}{\ln(9) - \ln(5)} \quad (2)$$

The above transformations are obtained by the following formula.

$$x = \frac{\ln(X_n) - \ln(X_{n0})}{\ln(X_{n1}) - \ln(X_{n0})} \quad (3)$$

where x is the coded value of any factor corresponding to its natural value X_n; X_{n1} is the natural value of the factor at the + level, and X_{n0} is the natural value of the factor corresponding to the base level or zero level.

IV. TESTS FOR ADEQUACY OF THE MODEL

The developed empirical model is confirmed for its adequacy using the following tests. Firstly, analysis of variance (ANOVA) is carried out for the quadratic response surface model and the statistics is given in the Table IV. It can be observed from Table IV that the value of "Prob. > F" for the model is less than 0.05, which indicates that the model is significant [13]. In the second, the multiple regression coefficient (R^2) is computed to check whether the fitted models actually describe the experimental data. The statistics of R^2 is defined as the ratio of variability explained by the model to the total variability in the actual experimental data and is used as a measure of goodness of fit [13]. If R^2 approaches to unity, the better the model fits the experimental data. In other words, it is the proportion of variation in the dependent variable (response) that can be explained by the predictors (factor) in the model. From Table IV, R^2 for Kw is found to be 0.9938. This shows that the second-order model can explain the variation in Kw up to the extent of 99.38%.

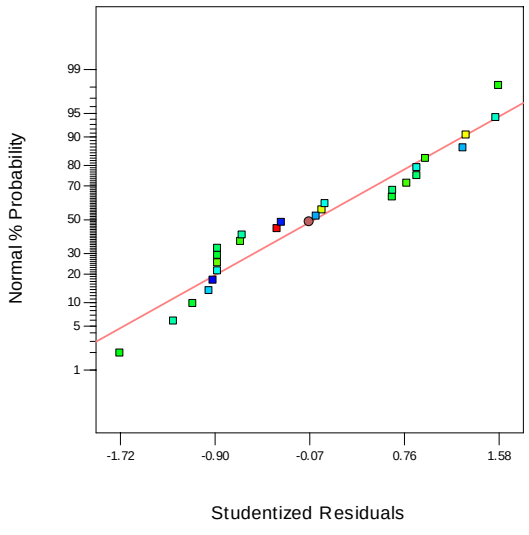

Fig. 3 Experimental setup for kerf measurement

From Table IV, adjusted R^2 for Kw is found to be 0.9770. It

can be observed that the values of R^2 and adjusted R^2 are much closer to each other. This proves that the developed model represent the process adequately. Thus, the developed mathematical model is checked for their adequacy using normal probability plot of residuals. The diagnostic plots are drawn to check whether the data is normally distributed and for any assumption is violated. In a normal probability plot, if all the data points fall near the line, an assumption of normality is reasonable. Otherwise, the points will curve away from the line, and an assumption of normality is not justified [13].

The normal probability plot of the residuals for the output response, Kw is shown in Fig. 3 and it can be observed that the residuals are located on straight line, which means that the errors are distributed normally.

TABLE IV
ANOVA [PARTIAL SUM OF SQUARES] FOR KW

Source	Sum of squares	d. f.	Mean square	F-value	Prob. > F
Model	0.014484	20	0.000724	48.3096	< 0.0001
X_1	0.000614	1	0.000614	40.9248	< 0.0007
X_2	0.002939	1	0.002939	196.044	< 0.0001
X_3	0.004548	1	0.004548	303.372	< 0.0001
X_4	9.05E-05	1	9.05E-05	6.03450	< 0.0494
X_5	0.000224	1	0.000224	14.9421	< 0.0083
X_1X_2	0.000152	1	0.000152	10.1255	< 0.0190
X_1X_3	7.51E-05	1	7.51E-05	5.00649	0.0666
X_1X_4	1.25E-05	1	1.25E-05	0.83455	0.3962
X_1X_5	1.11E-05	1	1.11E-05	0.74362	0.4216
X_2X_3	4.35E-05	1	4.35E-05	2.89860	0.1396
X_2X_4	0.000406	1	0.000406	27.0819	< 0.0020
X_2X_5	4.35E-05	1	4.35E-05	2.90096	0.1394
X_3X_4	6.24E-06	1	6.24E-06	0.41615	0.5427
X_3X_5	0.000172	1	0.000172	11.4483	< 0.0148
X_4X_5	2.9E-06	1	2.9E-06	0.19353	0.6754
X_1X_1	1.27E-05	1	1.27E-05	0.84892	0.3924
X_2X_2	8.38E-05	1	8.38E-05	5.59327	0.0559
X_3X_3	0.000143	1	0.000143	9.56491	0.0213
X_4X_4	3.86E-08	1	3.86E-08	0.00257	0.9612
X_5X_5	2.38E-05	1	2.38E-05	1.59035	0.2541
Residual	9.0E-005	7	1.287E-5		
Pure Error	5.5E-006	5	1.1E-006		
Cor Total	0.015	26			
Std. dev.	3.59E-03			R2	0.9938
Mean	0.33			Adj. R2	0.9733

< - refers to significant terms

V. ANALYSIS OF SIGNIFICANCE OF CONTROL VARIABLES

A. Main Effects

From the Table IV, it can be observed that the main effects of particulate size (X_1), percentage of the reinforcement(X_2), pulse-on time (X_3), pulse-off time (X_4) and wire tension (X_5) are significant on Kw. Also, the interactive effects of particulate size and percentage of the reinforcement (X_1X_2), percentage of the reinforcement and pulse-off time (X_2X_4) and pulse-on time and wire tension (X_3X_5) are significant.

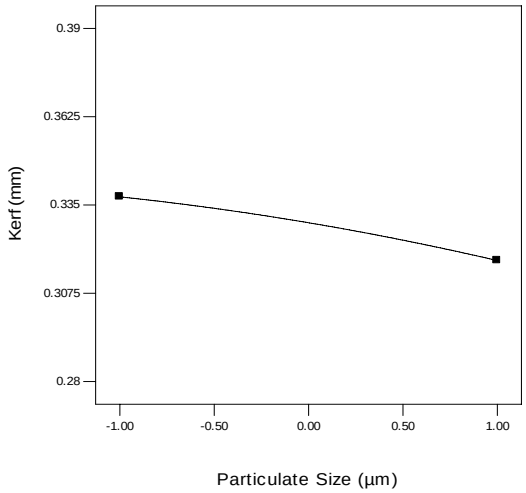

Fig. 4 Effect of particulate size on Kw

From Figs. 4 and 5, it is observed that the increased size and fraction of the particulate is considerably decreasing the Kw, due to the increased harness of the material with compacted and large particulate in the matrix. Fig. 6 shows that, the Kw is greatly affected by the pulse-on time, obviously it occurs that, the increased electric discharge energy caused to deeper and wider craters which widen the gap between the wire and the work piece. Fig. 7 shows that, the Kw is also affected by the pulse-off time but is in negative as compared to pulse-on time. Fig. 8 depicts the significance of wire tension on the Kw, the increasing trend of the Kw can be observed with increased wire tension due stabilized arc between the work piece and the tensed wire.

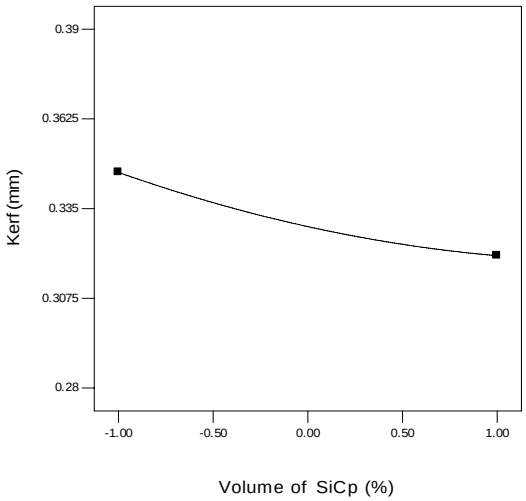

Fig. 5 Effect of volume fraction of SiC_P on Kw

B. Interaction Effects

Fig. 9 presents the interactive effects of particulate size and percentage of the reinforcement on Kw. The presence of hard SiC_P in the cutting path and the increased hardness due to increased size and addition of particulate are the reasons for

decreasing the kerf. From Fig. 10, it is obvious that for the higher volume of reinforcement in combination with increased pulse-off time reduces the kerf. However, the combined effect of increased pulse-on time and wire tension causing to increase the Kw greatly as shown in Fig. 11.

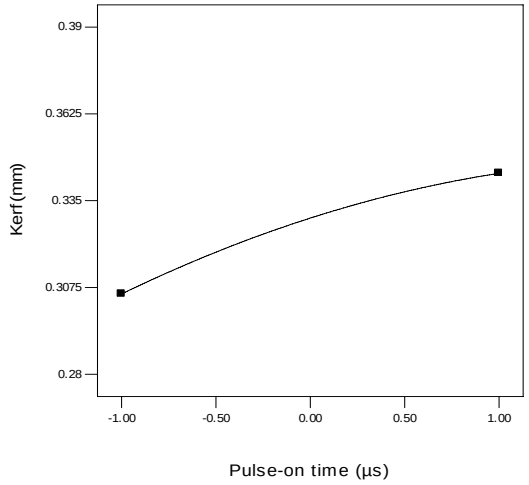

Fig. 6 Effect of pulse-on time on Kw

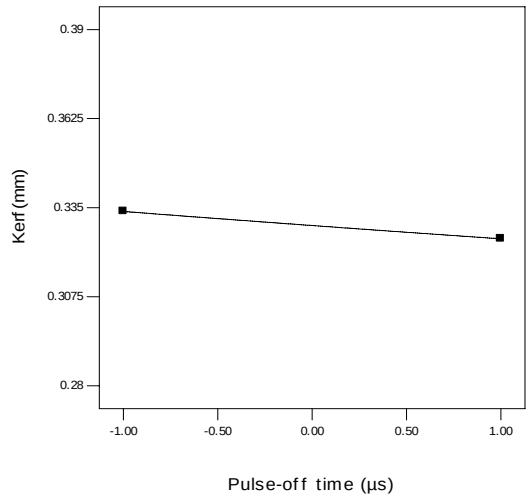

Fig. 7 Effect of pulse-off time on Kw

VI. Formulation of Optimization Problem

In order to optimize the measured response, the problem is formulated as single objective optimization problem of minimization of kerf subjected to the boundaries of the variables varied in the machining experiments. The problem is formulated as follows:

To find: X_1, X_2, X_3, X_4 and X_5 (4)

Minimize:

$$\begin{aligned} Kw = {} & 0.33 - 0.0099x_1 - 0.013x_2 + 0.019x_3 - 0.0042x_4 \\ & + 0.0064x_5 - 0.0019x_1^2 + 0.0038x_2^2 - 0.0049x_3^2 \\ & + 0.0002x_4^2 - 0.0036x_5^2 + 0.0047x_1x_2 - 0.0041x_1x_3 \\ & - 0.0029x_1x_4 - 0.0024x_1x_5 - 0.0026x_2x_3 - 0.0065x_2x_4 \\ & - 0.0025x_2x_5 + 0.0009x_3x_4 - 0.0053x_3x_5 + 0.0012x_4x_5 \end{aligned} \quad (5)$$

Subjected to,

$$25\ \mu m \le X_1 \le 75\ \mu m \quad (6)$$

$$5\ \% \le X_2 \le 10\ \% \quad (7)$$

$$5\ \mu s \le X_3 \le 9\ \mu s \quad (8)$$

$$25\ \mu s \le X_4 \le 45\ \mu s \quad (9)$$

$$1\ gms \le X_5 \le 9\ gms \quad (10)$$

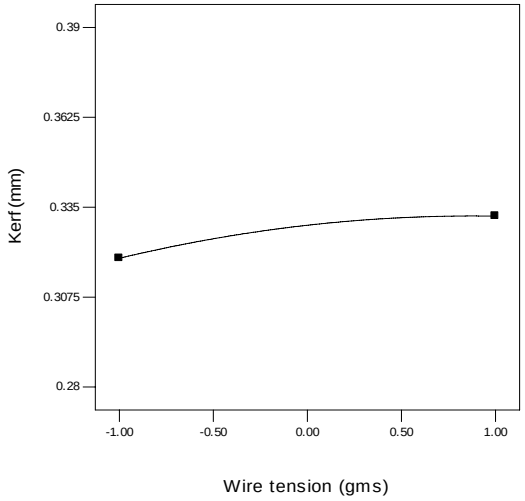

Fig. 8 Effect of wire tension on Kw

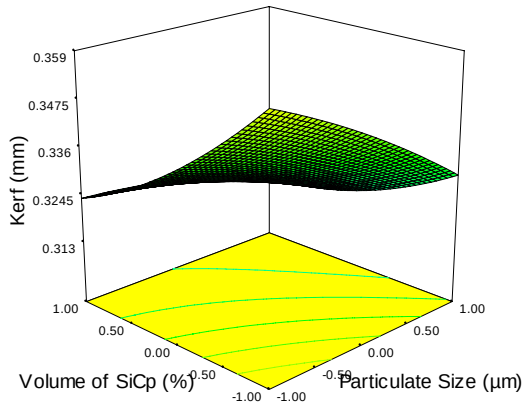

Fig. 9 Interactive effect of particulate size and volume fraction of SiC_P on Kw

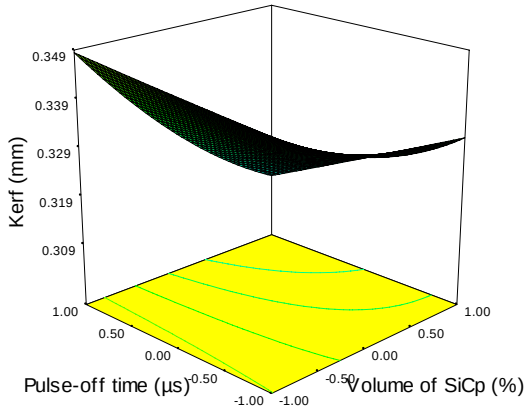

Fig. 10 Interactive effect of volume fraction of SiC_P and pulse-off time on Kw

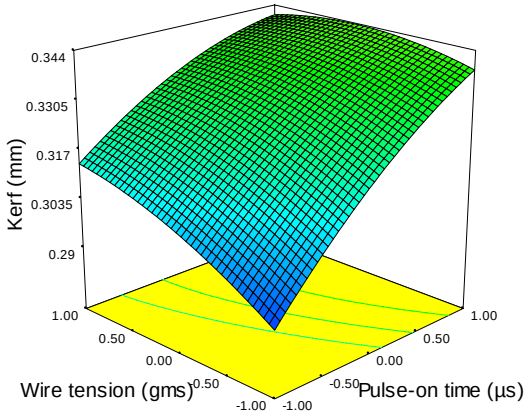

Fig. 11 Interactive effect of pulse-on time and wire tension on Kw

VII. Optimization Using GA

Application of genetic algorithms is idyllic approach for the complex multi-variable optimization problems [14]. GA as non-traditional optimization methods are being successfully implemented for variety of the manufacturing applications [15]. Palanisamy et al. [16] implemented GA to find the optimum machining parameters for end-milling operations. They highlighted the accuracy and effectiveness of the GA based on the good agreement between the GA results and the experimentally validated results in this investigation. The methodology of the GA begins with generation of a set of strings (or chromosomes) randomly called population. Traditionally, a binary coding system is adopted to represent the chromosomes in terms of either zeros or ones. After, the fitness values (objective function value) are computed for each member in the population, three fundamental GA operators called reproduction, cross over and mutation are operated on the population to create a now population also called child population. The child population is further evaluated and tested for determination with reference to the parent population. In the simulation of GA, one iteration of these three operators is named as a generation [17].

In this investigation, GA is implemented to the formulated objective function to find the global minimum value of kerf. The implementation of GA is clearly explained in Tables V-VII for minimizing the Kw as objective. One iteration of the algorithm, the sample calculations are presented here. The bit lengths of 5, 4, 4, 3 and 3 are chosen for X_1, X_2, X_3, X_4 and X_5 respectively. The initial population with 27 chromosomes is randomly generated as a first step of the algorithm and is shown in Table V. The decoded decimal values of Kw of the generated chromosome strings of individual input variables are listed in Table V. For example, from Table V, the first string (10011 1111 1101 000 111) is decoded to values equal to X_1=56; X_2=15; X_3=8; X_4=25; X_5=9 using linear mapping rule as presented in (11).

$$x_i = X_i^L + \frac{X_i^U - X_i^L}{2^{l_i} - 1} \times decoded\ value \tag{11}$$

Then the objective function Kw value is computed which is obtained as 0.3357. The fitness function value at this point using the transformation rule F(x(1)) = 1.0 /(1.0+0.3357) is obtained as 0.7486. This fitness function value is used in the reproduction operation of GA.

TABLE V
Initial Population with Fitness Values in GA

S. No.	Chromosomes					X_1	X_2	X_3	X_4	X_5	Kw	Fitness value
1	10011	1111	1101	000	111	56	15	8	25	9	0.336	0.749
2	10111	1101	0011	011	000	62	14	6	34	1	0.299	0.770
3	11000	0100	1111	101	100	64	8	9	39	6	0.339	0.747
4	11001	0110	0101	000	001	65	9	6	25	2	0.313	0.762
5	10101	0010	1100	110	001	59	6	8	42	2	0.338	0.747
6	11010	1001	0010	000	010	67	11	6	25	3	0.305	0.766
7	11101	1011	0110	100	001	72	12	7	36	2	0.306	0.766
8	01111	1111	1000	001	101	49	15	7	28	7	0.328	0.753
9	10011	0000	1101	010	111	56	5	8	31	9	0.357	0.737
10	10001	1101	0011	110	011	52	14	6	42	4	0.298	0.770
11	10100	0110	0101	001	101	57	9	6	28	7	0.325	0.755
12	10011	0101	0101	010	010	56	8	6	31	3	0.318	0.759
13	10101	1101	0011	111	101	59	14	6	45	7	0.299	0.770
14	11111	0111	0001	000	111	75	10	5	25	9	0.312	0.762
15	11001	1100	1100	011	001	65	13	8	34	2	0.323	0.756
16	10011	1111	0011	010	101	56	15	6	31	7	0.313	0.762
17	11001	0011	1100	101	010	65	7	8	39	3	0.334	0.750
18	10101	1010	1010	000	111	59	12	8	25	9	0.335	0.749
19	01010	0101	1110	100	001	41	8	9	36	2	0.345	0.743
20	11000	1100	0011	111	001	64	13	6	45	2	0.291	0.775
21	11001	1011	1001	100	001	65	12	7	36	2	0.315	0.760
22	10001	1101	0110	001	110	52	14	7	28	8	0.326	0.754
23	11011	0101	0011	101	011	69	8	6	39	4	0.307	0.765
24	10011	1100	1011	011	011	56	13	8	34	4	0.325	0.755
25	00100	0010	0010	110	001	31	6	6	42	2	0.316	0.760
26	00011	0011	0110	001	010	30	7	7	28	3	0.336	0.749
27	11101	0110	1111	000	001	72	9	9	25	2	0.334	0.750

Similarly, other strings in the population are evaluated and fitness values are calculated. Table V shows the objective function value and the fitness value for all the 27 strings in the initial population. In the next step, good strings in the

population are to be selected to form the mating pool. In this work, roulette-wheel selection procedure is used to select the good strings. As a part of this procedure, average fitness of the population is calculated by adding the fitness values of all strings and dividing the sum by the population size and the average fitness of the population $(\bar{F})$ is obtained as 0.7570.

The expected count is subsequently calculated by dividing each fitness value with the average fitness, $(F(x)/\bar{F})$. For the first string, the obtained expected count is (0.7486/0.7570)= 0.989. Similarly, the expected count values are calculated for all other strings in the population and shown in Table VI. Then, the probability of each string being copied in the mating pool can be computed by dividing the expected count values with the population size. For instance, the probability of first string is (0.989/27) = 0.037. Similarly, the values of probability of selection for all the strings are calculated and cumulative probability is henceforward computed. The probabilities of selection are listed in Table VI.

TABLE VI
SELECTION IN GA

S. No.	Expected Count	Probability	Cumulative Probability	Random number	Selected String number
1	0.989	0.037	0.037	0.225	6
2	1.017	0.038	0.074	0.721	20
3	0.987	0.037	0.111	0.346	9
4	1.006	0.037	0.148	0.354	10
5	0.987	0.037	0.185	0.887	24
6	1.012	0.037	0.222	0.493	13
7	1.011	0.037	0.260	0.329	8
8	0.994	0.037	0.296	0.086	2
9	0.973	0.036	0.332	0.044	1
10	1.018	0.038	0.370	0.687	18
11	0.997	0.037	0.407	0.650	17
12	1.002	0.037	0.444	0.084	2
13	1.017	0.038	0.482	0.032	1
14	1.007	0.037	0.519	0.886	24
15	0.998	0.037	0.556	0.536	15
16	1.006	0.037	0.593	0.840	23
17	0.990	0.037	0.630	0.732	20
18	0.990	0.037	0.667	0.281	8
19	0.982	0.036	0.703	0.869	23
20	1.024	0.038	0.741	0.882	24
21	1.004	0.037	0.778	0.125	4
22	0.996	0.037	0.815	0.421	11
23	1.011	0.037	0.853	0.913	25
24	0.997	0.037	0.890	0.538	14
25	1.004	0.037	0.927	0.393	11
26	0.989	0.037	0.963	0.272	7
27	0.991	0.037	1.000	0.034	1

TABLE VII
CROSSOVER AND MUTATION IN GA (MINIMIZATION OF KW)

Selection	Mating pool					Cross over?	Cross-over site	Offspring					Mutation sites	Mutated chromosome				
6	11010	1001	0010	000	010	NO	--	11010	1001	0010	000	010	--	11010	1001	0010	000	010
20	11000	1100	0011	111	001	NO	--	11000	1100	0011	111	001	8	11000	1110	0011	111	001
9	10011	0000	1101	010	111	NO	--	10011	0000	1101	010	111	--	10011	0000	1101	010	111
10	10001	1101	0011	110	011	NO	--	10001	1101	0011	110	011	--	10001	1101	0011	110	011
24	10011	1100	1011	011	011	YES	9,16	10011	1100	0011	111	011	--	10011	1100	0011	111	011
13	10101	1101	0011	111	101	YES	9,16	10101	1101	1011	011	101	--	10101	1101	1011	011	101
8	01111	1111	1000	001	101	NO	--	01111	1111	1000	001	101	2,10	00111	1111	0000	001	101
2	10111	1101	0011	011	000	NO	--	10111	1101	0011	011	000	--	10111	1101	0011	011	000
1	10011	1111	1101	000	111	NO	--	10011	1111	1101	000	111	--	10011	1111	1101	000	111
18	10101	1010	1010	000	111	NO	--	10101	1010	1010	000	111	--	10101	1010	1010	000	111
17	11001	0011	1100	101	010	NO	--	11001	0011	1100	101	010	--	11001	0011	1100	101	010
2	10111	1101	0011	011	000	YES	5,9	10111	1111	0011	011	000	5	10110	1111	0011	011	000
1	10011	1111	1101	000	111	YES	5,9	10011	1101	1101	000	111	--	10011	1101	1101	000	111
24	10011	1100	1011	011	011	NO	--	10011	1100	1011	011	011	--	10011	1100	1011	011	011
15	11001	1100	1100	011	001	NO	--	11001	1100	1100	011	001	7,3	11101	1000	1100	011	001
23	11011	0101	0011	101	011	NO	--	11011	0101	0011	101	011	--	11011	0101	0011	101	011
20	11000	1100	0011	111	001	NO	--	11000	1100	0011	111	001	--	11000	1100	0011	111	001
8	01111	1111	1000	001	101	NO	--	01111	1111	1000	001	101	--	01111	1111	1000	001	101
23	11011	0101	0011	101	011	NO	--	11011	0101	0011	101	011	--	11011	0101	0011	101	011
24	10011	1100	1011	011	011	YES	9,13	10011	1100	0101	011	011	--	10011	1100	0101	011	011
4	11001	0110	0101	000	001	YES	9,13	11001	0110	1011	000	001	8,15	11001	0100	1011	010	001
11	10100	0110	0101	001	101	NO	--	10100	0110	0101	001	101	--	10100	0110	0101	001	101
25	00100	0010	0010	110	001	NO	--	00100	0010	0010	110	001	--	00100	0010	0010	110	001
14	11111	0111	0001	000	111	NO	--	11111	0111	0001	000	111	--	11111	0111	0001	000	111
11	10100	0110	0101	001	101	NO	--	10100	0110	0101	001	101	--	10100	0110	0101	001	101
7	11101	1011	0110	100	001	NO	--	11101	1011	0110	100	001	--	11101	1011	0110	100	001
1	10011	1111	1101	000	111	NO	--	10011	1111	1101	000	111	--	10011	1111	1101	000	111

TABLE VIII
OPTIMUM MACHINING CONDITIONS FOR KW

Control factors and responses	Optimum value	
	GA	Experimental
Particulate size (μm)	65.84	65.00
%volume of SiCP	14.32	14.32
Pulse-on time (μs)	5.00	5.00
Pulse-off time (μs)	44.85	44.85
Wire tension (gm)	1.00	1.00
Kw (mm)	0.272	0.274

Now, random numbers between zero and one are generated in order to form the mating pool. From Table VI, random number generated for the first string is 0.225 which means the sixth string from the population gets a copy in the mating pool, because that string occupies with the probability interval (0.222, 0.260) as shown in the column of cumulative probability in the Table VI. In a similar manner, other strings are selected according to the random numbers generated in Table VI and the complete mating pool is formed. The mating pool is displayed in Table VII. By adopting the reproduction operator, the inferior points have been automatically eliminated from further consideration.

TABLE IX
VALIDATION OF MODEL

Exp No.	Machining conditions					Kw (mm)		
	Size of SiC_P (μs)	Volume of SiC_P (%)	Pulse-on time (μs)	Pulse-Off time (μs)	Wire tension (gm)	Predicted	Experiment	Deviation (%)
1	25	7	5	29	1	0.3011	0.3012	0.03470
2	50	10	8	26	6	0.3398	0.3398	0.00523
3	75	13	9	42	3	0.3162	0.3163	0.02880
4	50	8	6	30	6	0.3244	0.3246	0.06165
5	75	11	7	40	3	0.3091	0.3101	0.32351
6	25	13	8	38	7	0.3372	0.3393	0.61196
7	75	15	9	35	9	0.3149	0.3150	0.04132
8	25	3	7	37	5	0.3697	0.3705	0.21755
9	50	6	7	39	3	0.3336	0.3336	0.00000
10	25	5	6	27	6	0.3471	0.3486	0.42943
11	75	9	7	41	9	0.3198	0.3184	0.44530
12	50	12	9	42	7	0.3298	0.3299	0.03033
13	25	10	5	32	4	0.3065	0.3085	0.65260
14	50	14	6	37	3	0.3025	0.3026	0.03205
15	75	15	5	35	5	0.2939	0.2959	0.68043
16	25	8	8	38	8	0.3618	0.3619	0.02223
17	75	9	7	25	4	0.3193	0.3195	0.06263
18	50	6	6	30	2	0.3166	0.3168	0.06317

As a next step in the generation, the strings in the mating pool are used for the crossover operation. In the crossover operation, two strings are selected at random and crossed at a random site. Since the mating pool contains strings at random, pairs of strings are picked-up from top of the list as shown in Table VII. Thus strings 6 and 20 participate in the first crossover operation. In this work, two-point crossover [18] is adopted with the probability, pc=0.85 to check whether a crossover is desired or not. To perform crossover, a random number is generated with crossover probability (pc) of 0.85. If the random number is less than pc then the crossover operation is performed, otherwise the strings are directly placed in an intermediate population for subsequent genetic operation. When crossover is required to be performed then crossover sites are to be decided at random by creating random numbers between (0, *l*-1), where l represents the total length of the string. For example, when crossover is required to be performed for the strings 24, 13 two sites of crossover are to be selected randomly. Here, the random sites are happened to be 9, 16. Thus the portions between sites 9 and 16 of the strings 24 and 13 are swapped to create the new offspring as shown in Table VII. However, with the random sites, the children strings produced may or may not have a combination of good strings from parent strings, depending on whether or not the crossing sites fall in the appropriate locations. If good strings are not created by crossover, they will not survive too long because reproduction will select against those chromosomes in subsequent generations. In order to preserve some of the good chromosomes that are already present in the mating pool, all the chromosomes are not used in crossover operation. When a crossover probability of p_c is used, the expected number of strings that will be subjected to crossover is only $100p_c$ and the remaining percent of the population remains as they are in the current population. The calculations of intermediate population are shown in the Table VII. The crossover is mainly responsible for the creation of new strings.

The third operator, mutation, is then applied on the intermediate population. Mutation is basically intended for local search around the current solution. Bit-wise mutation is performed with a probability, p_m=0.10. A random number is generated with p_m; if random number is less than p_m then the bit is altered from 1 to 0 or 0 to 1 depending on the bit value otherwise no action is taken. Mutation is implemented with

the probability, p_m=0.10 as shown in Table VII. The procedure is repeated for all the strings in the intermediate population. This completes one iteration of the GA. The above procedure is continued until the maximum number of generations is completed. For better convergence, the algorithm is run for 500 generations.

VIII. Results and Discussions

In order to find the optimal set of machining parameters which results the best global minimum value of Kerf, the MATLAB GA tool box is used to simulate the algorithm. One of the major advantages with GA is that it the users need not supply any supporting information excluding the objective function values and constraints. In addition, no assumptions are to be made while applying the algorithm and it works with a population of points instead of a single point, thus the expected solution may be a global solution. GA narrows down the search space as the search progresses.

In the present problem, GA is run for 500 generations and the algorithm is converged to the objective function value of 0.272. The fitness value convergence graph is displayed in Fig. 12 and the optimal values of the control factors are listed in Table VIII. The following results are resolved from the simulation results from the proposed methodology: From the experimental observations Table III the least kerf value measured is 0.282 for the 13th experiment, However, after optimization using GA, it is observed from Table VIII that Kw is decreased to 0.276 mm it means around 3.546% of the kerf value can be minimized by adopting the machining control variables listed in Table VIII. However, to check the practical possibility of the obtained optimal process parameters, the validation experiment was conducted on the same experimental setup to measure kerf. The result obtained from the GA and validation test were correlated as presented in Table VIII.

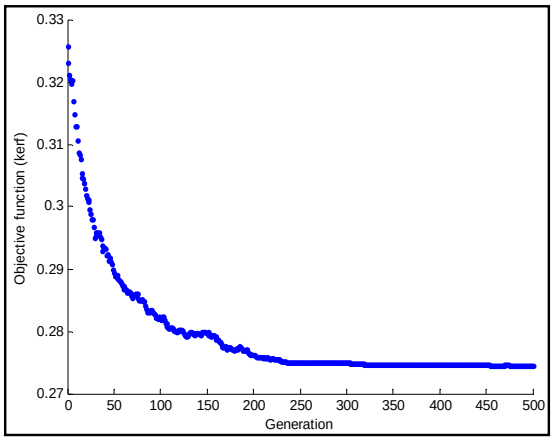

Fig. 12 Convergence graph for minimization of Kw

IX. Confirmation Experiments

The next step to the optimization is the experimental validation of the obtained results of the proposed method. Therefore, the conformation experiments are conducted to validate the predicated response surface model of the Kerf. The values of the control variables are selected within the upper and lower limit values used for experimentations in the design matrix and to derive the models.

The same experimental setup is used to conduct the validation tests in the manufacturing facility. Total eighteen confirmation experiments are performed with distinct parameters settings and the measured Kw values are listed in Table IX. A comparative study between the predicted and experimental results is carried out and furnished in Table IX.

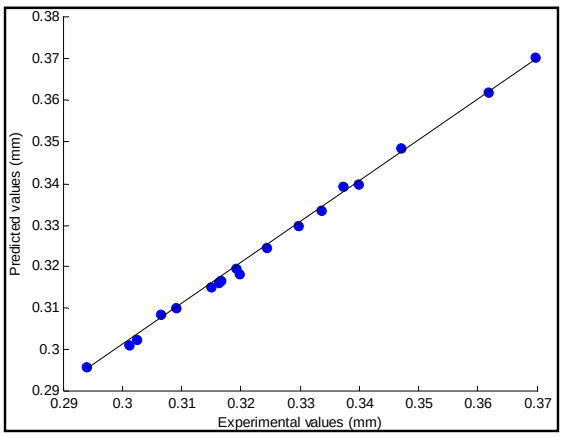

Fig. 13 Predicted values vs. experimental values for Kw

Fig. 13 shows the one-to-one plots drawn between the predicted values and the experimental values. It is observed from the figures that the proposed methodology ensures the reasonable predictions and it can be concluded that the developed mathematical models have good agreements with the experimental test lines. Slight variations between the results might be due to the random factors like probable material defects and minute tool deflection from its mean position because of electrodynamics forces on the wire.

X. Conclusions

With the aim of precise machining of metal matrix composites in wire electrical discharge machining, the optimal settings of the control variables are determined which results globally best kerf during machining SiC_P reinforced Al7075 MMCs. The experimental runs are conducted on stir casted Al7075/SiC_P MMCs of three levels SiC particulate size viz., 25, 50 and 75µm and are at 5, 10 and 15% of volume of the matrix.

Based on the Taguchi's orthogonal array the experiments are designed. During the experimentations, the most significant processes parameters of WEDM process of pulse-on time, pulse-off time and wire tension are used as machining variables along with the particulate size and volume fraction of the SiC_P in the work piece to measure the kerf as the process response.

Based on the experimental measurements, an empirical model was derived by using response surface methodology

and is confirmed for its adequacy to represent the experimental results. Also the model is validated within the bounds of the process variables. It facilitates to predict the kerf in WEDM helps in process optimization. Consequently, GA is used to determine the optimal parameters which reduced the kerf to 0.272 mm. Hence, with the GA-based optimization system developed to machine Al7075/SiC_P using WEDM would improve the machining efficiency by 3.546% using optimal cutting parameters. Also the proposed methodology could helps to automate the machining system at the computer aided process planning (CAPP) stages to produce high quality components of Al7075/SiC_P MMCs with tight tolerances by WEDM.

REFERENCES

[1] M. Rosso, Ceramic and metal matrix composites: Routes and properties, Journal of Materials Processing Technology 175 (2006) 364–375.
[2] A. Manna Æ B. Bhattacharyya, Investigation for optimal parametric combination for achieving better surface finish during turning of Al /SiC-MMC, Int J Adv Manuf Technol (2004) 23: 658–665.
[3] Harlal Singh Mali, Alakesh Manna, Simulation of surface generated during abrasive flow finishing of Al/SiC p -MMC using neural networks, Int J Adv Manuf Technol (2012) 61:1263 – 1268.
[4] Ho KH, Newman ST, Rahimifard S, Allen RD (2004) State of the art in wire electrical discharge machining (WEDM). Int J Mach Tools Manuf 44:1247 – 1259.
[5] C. Satishkumar, M. Kanthababu, V. Vajjiravelu, R. Anburaj, N. Thirumalai Sundarrajan, H. Arul, Investigation of wire electrical discharge machining characteristics of Al6063/SiC p composites, Int J Adv Manuf Technol (2011) 56:975 – 986.
[6] Guo ZN, Wang X, Huang ZG, Yue TM (2002) Experimental investigation into shaping particles-reinforce material by WEDM HS. J Mater Process Technol 129:56 – 59.
[7] Yan BH, Tsai HC (2005) Examination of wire electrical discharge machining of Al_2O_3/6061Al composites. Int J Mach Tools Manuf 45(3):251 – 259.
[8] Aniza Alias, Bulan Abdullah, Norliana Mohd Abbas, Influence of machine feed rate in wedm of titanium Ti-6Al-4V with constant current (6a) using brass wire, Procedia Engineering, 41, (2012), 1806 – 1811.
[9] Kodalagara Puttanarasaiah Somashekhar & Nottath Ramachandran & Jose Mathew, Material removal characteristics of microslot (kerf) geometry in μ-WEDM on aluminium Int J Adv Manuf Technololgy, 2010, 51:611–626.
[10] Sangju Lee, Michael A. Scarpulla, Eberhard Bamberg, Effect of metal coating on machinability of high purity germanium using wire electrical discharge machining, Journal of Materials Processing Technology 213 (2013) 811–817.
[11] Nihat Tosun, Can Cogun and Gul Tosun, 2004, A study on kerf and material removal rate in wire electrical discharge machining based on Taguchi method, Journal of Materials Processing Technology – Journal of material processing and technology, vol. 152, no. 3, pp. 316-322, 2004.
[12] K. Palanikumar, R. Karthikeyan, Optimal machining conditions for turning of particulate metal matrix composites using Taguchi and response surface methodologies, Machining Science and Technology: An International Journal, 10:417–433.
[13] Montgomery, D. C., "Design and analysis of experiments", 5th edition, *John Wiley & Sons, INC*, New York, 2003.
[14] Chen CJ, Tseng CS (1996) The path and location planning of workpiece by genetic algorithms. J Intell Manuf 7:69.
[15] Dereli T, Filiz IH, Baykasoglu A (2001) Optimizing cutting parameters in process planning of prismatic parts using genetic algorithms. Int J Prod Res 39:3303.
[16] P. Palanisamy, I. Rajendran, S. Shanmugasundaram, Optimization of machining parameters using genetic algorithm and experimental validation for end-milling operations, International Journal of Advanced Manufacturing Technology, 32: (2007) 644 – 655.
[17] Kalyanmoy Deb, Optimization for engineering design: Algorithms and Examples, PHI Learning Limited, New Delhi, 2010.
[18] Deb, K., "Multi objective optimization using evolutionary algorithms", *John Wiley & Sons (ASIA) Pte. Ltd*., Singapore, 2001.